

# Estimation of Local Conduction Velocity from Myocardium Activation Time: Application to Cardiac Resynchronization Therapy

Thomas Pheiffer<sup>1</sup>, David Soto-Iglesias<sup>2,3</sup>, Yaroslav Nikulin<sup>1</sup>,  
Tiziano Passerini<sup>1</sup>, Julian Krebs<sup>1</sup>, Marta Sitges<sup>3</sup>, Antonio Berruezo<sup>3</sup>,  
Oscar Camara<sup>2</sup>, and Tommaso Mansi<sup>1</sup>(✉)

<sup>1</sup> Siemens Medical Solutions, Medical Imaging Technologies, Princeton, NJ, USA  
tommaso.mansi@siemens.com

<sup>2</sup> Universitat Pompeu Fabra, Barcelona, Spain

<sup>3</sup> Cardiology Department, Thorax Institute, Hospital Clinic, Barcelona, Spain

**Abstract.** As models of cardiac electrophysiology (EP) are maturing, an increasing effort is being put in their translation to the bed side, in particular for abnormal cardiac rhythm diagnosis and therapy planning. However, the parameters that govern these models need to be estimated from noisy and sparse clinical data in an efficient and precise way, which is still an unsolved challenge. Invasive cardiac mapping provides the richest EP information available today. This paper proposes a new method to estimate a local map of electrical conductivities of the bi-ventricular heart by applying the back-propagation error concept, widely used in neural networks. The method works when either endocardial or epicardial activation time maps are available, and can cope with heterogeneous cardiac tissue. The method was evaluated on synthetic data, showing significantly increased performance in goodness of fit compared to a global parameter estimation approach. The resulting predictive power of the personalized model for cardiac resynchronization therapy was then assessed on 16 swine models of left bundle branch block with rich imaging and EP data before and after CRT. With the proposed personalization, the average error in activation time post CRT was  $10 \pm 4.5$  ms, lower than the observed pre/post-CRT difference of  $26.3 \pm 16.8$  ms.

## 1 Introduction

Computational models of cardiac electrophysiology (EP) are reaching a level of maturity that enables the development of new tools to support clinical management of cardiac rhythm diseases. Application to atrial or ventricular arrhythmias [1], bundle branch blocks [12], ablation therapy [2] and cardiac resynchronization therapy (CRT) [10] have been explored. Yet, one crucial challenge that still needs to be addressed is the efficient, robust and precise estimation of the parameters that govern the equations associated to EP models, so as to individualize them and capture the specific patho-physiology of the patient under

consideration [3]. Due to the sparsity and noisy nature of clinical data (imaging, ECG or, in the best case, electro-anatomical mappings (EAM)), not all the parameters can be observed and assumptions are required. Also, due to the computational burden, only a few parameters are estimated and uniformity assumptions, or even default values determined from animal experiments, are often used [5, 6, 11].

This paper focuses on the estimation of local, point-wise conduction velocities within the bi-ventricular myocardium from activation maps. Several approaches have been proposed in the past, including coarse-to-fine optimization [8] or with uncertainty quantification [15]. A comprehensive review can be found in [3]. Yet, the local estimation of the conduction velocity remains a challenge due to the high number of unknown variables and computational demand.

Inspired by neural network theories [4], we propose a novel, back-propagation technique to estimate the electrical conductivity along the edges of a volumetric mesh representing the bi-ventricular myocardium (Sect. 2). The approach assumes a front propagation without re-entry and the availability of at least one of endo- and epi-cardial maps of local activation times (LAT). Given measured LAT and a graph-based model of cardiac EP, the errors between simulated and measured LATs are iteratively propagated back with respect to the front-wave to adjust the conduction velocities of every edge of the mesh. The approach copes with different tissue types and anisotropy. The method was verified on synthetic data (Sect. 3). The algorithm performance in predicting the electrical response of CRT was then evaluated on 16 comprehensive swine datasets, showing promising generalization performance. Section 4 concludes the paper.

## 2 Methods

### 2.1 Forward Model of Cardiac Electrophysiology

**Anatomical Model.** The anatomical model is estimated following the framework described in [6]. In brief, machine learning algorithms are employed to efficiently segment the left (LV) and right (RV) ventricle endocardia and LV epicardium from cine MRI. The surfaces are then fused together and a volumetric tetrahedral mesh created. By leveraging the point-correspondences of the segmented meshes, myocardium fibers and mesh tags (LV/RV septum, LV/RV endocardium) are defined automatically (Fig. 1).

**EP Model.** The resulting volumetric mesh defines the computational domain for solving the EP equations to get point-wise LATs. This work relies on a graph-based EP model, termed GraphEP, in which the LAT at each point of the mesh is calculated given LV, RV septal and device activation points using a shortest-path algorithm adapted to the EP use case [6, 14, 15]. A generalized edge weight is calculated such that the conduction velocity along each edge takes into account the different tissues it traverses and the local anisotropy. Let  $\mathbf{p}_i$  and  $\mathbf{p}_j$  be two connected mesh points. The generalized edge weight  $w_{ij}$ , measured in seconds, corresponds to the time needed for the action-potential to travel from  $\mathbf{p}_i$  to  $\mathbf{p}_j$ :

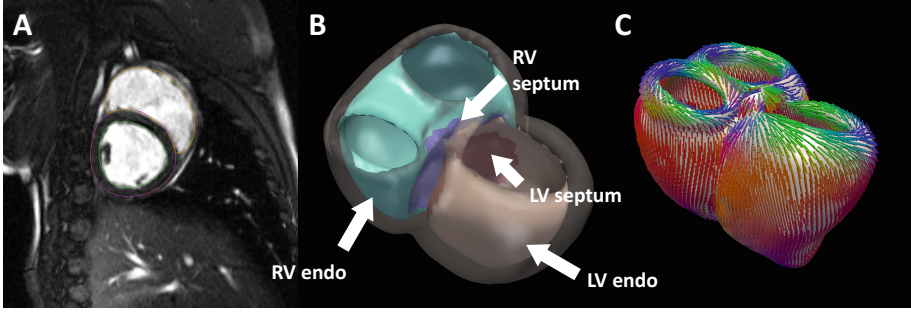


**Fig. 1.** Left: MR image volume from which the cardiac structures are segmented. Middle: segmentation of the heart structures as a transparent mesh. Right: anatomical model used for the computation, with color lines representing myocardium fibers.

$w_{ij} = l_{ij}/c_{ij}$ , where  $l_{ij} = \sqrt{(\mathbf{e}_{ij}^T \mathbf{D} \mathbf{e}_{ij})}$ ,  $\mathbf{e}_{ij} = \mathbf{p}_i - \mathbf{p}_j$ ,  $\mathbf{D}$  is the anisotropy tensor defined as  $\mathbf{D} = (1 - r)\mathbf{f}_{ij}\mathbf{f}_{ij}^T + r\mathbf{I}$ ,  $\mathbf{f}_{ij}$  is the fiber direction along the edge and  $r$  the anisotropy ratio ( $r = 0.3$ ).  $c_{ij}$  is the apparent conduction velocity in m/s along the edge approximated linearly from the conduction velocity  $c_i$  and  $c_j$  and the different tissue types the edge traverses. In other words, the EP model is essentially a Dijkstra shortest path propagation of activation time along the mesh edges, in which the cost is controlled by the parameters described here.

**EP Activation Model.** Intrinsic cardiac stimulation is modeled by an instantaneous activation of the LV and RV septum, to mimic the effects of the His bundle. In terms of the Dijkstra graph model, this means setting the point-wise activation time to zero on these mesh regions. Fast activation from the Purkinje network is modeled assigning different conduction velocity to a smooth, thin layer of nodes distributed all over the endocardial surfaces of the LV and RV ( $c_{LV}$  and  $c_{RV}$ ). The thickness of this fast conducting layer is set to 3 mm to model swine Purkinje system, which goes deeper within the myocardium than in humans. With these conditions and material properties set, the shortest-path propagation is calculated to obtain the full EP activation across the heart.

## 2.2 Local Estimation of Conduction Velocities

Electro-anatomical mapping data (EAM) is integrated with the MRI surface using a quasi-conformal mapping technique (QCM). QCM takes advantage of the existence of a homeomorphism between the LV endocardial surface and a 2D disk. By mapping both MRI and EAM surfaces to the same disk we can easily establish a piecewise linear homeomorphism between the two surfaces, as in [13].

The personalization algorithm is initialized by estimating three conduction velocities ( $c_{LV}$ ,  $c_{RV}$  and  $c_{Myo}$ ) that minimize the sum of squared distances (SSD) between measured and simulated LATs at the points where measurement is available. These three values are the velocity in the Purkinje layer of the left ventricle, in the Purkinje layer of the right ventricle, and in the myocardium, respectively.

This initialization step is hereafter referred to as the global personalization step, as these conduction velocities are merely estimated as a single value for each particular tissue region. Formally, the SSD objective is defined as:

$$D = \sum_{i=0}^N (m_i - c_i)^2 \quad (1)$$

where  $m_i$  is the measured activation time at point  $i$ , and  $c_i$  is the calculated activation time at point  $i$ . The distance is calculated over all the  $N$  points where measured activation time data is available. Note that the conduction velocities could be calculated volumetrically, e.g. just on the edges. We chose a point-wise implementation primarily for ease of integration in the rest of our data processing workflow, particularly for visualization purposes. Point-wise conductivities also allow modeling an apparent conductivity when the edge crosses different tissue types. A standard, trust-region technique is employed [7]. Next, the generalized edge weights are estimated  $w_{ij}$ . Let  $\mathcal{L}$  be the loss between measured and computed LATs,  $\mathcal{L} = \sum_{i=0}^N (t_{m,i} - t_{c,i})^2$ , where  $N$  is the total number of points where measurement is available,  $t_{m,i}$  and  $t_{c,i}$  are the measured and computed activation times at point  $i$ , respectively. If the EP wave propagates without re-entries, one can see the mesh nodes arranged in layers approximatively parallel to the EP iso-chrones, similar to a neural network layer. The input layer is thus the set of activation points, and the output layer can be defined as the set of nodes where LAT measurement is available, to enable back-propagation parameter estimation. Thus after the initial global personalization, we seek to personalize the point-wise conductivities based on back-propagation along the edges until the error at the data points reaches a convergence tolerance. The edges which are not reached by the backpropagation algorithm keep their conductivity values assigned during the global personalization. A variant of gradient descent with step  $\alpha$  is used to adjust the generalized edge weights  $w_{ij}$  so as to minimize  $\mathcal{L}$ :  $w'_{ij} = w_{ij} - \alpha \frac{\partial \mathcal{L}}{\partial w_{ij}}$ . Assuming that the LAT at point  $j$  is known, the partial derivative can be written as:

$$\frac{\partial \mathcal{L}}{\partial w_{ij}} = \frac{\partial \mathcal{L}}{\partial t_{c,j}} \frac{\partial t_{c,j}}{\partial w_{ij}} \quad (2)$$

As a property of the backpropagation framework implemented on the mesh graph, the edge weight  $w_{ij}$  only effects the overall loss function  $\mathcal{L}$  based on its affect on the output at point  $j$ . Note that this statement follows from the perspective of the personalization step, in which the errors are propagated backwards rather than forward. Thus, Eq. 2 writes:

$$\frac{\partial \mathcal{L}}{\partial w_{ij}} = -2(t_{m,j} - t_{c,j}) \frac{\partial t_{c,j}}{\partial w_{ij}}$$

Exploiting the fact that the solution is a shortest path solution, the second term becomes:

$$\frac{\partial t_{c,j}}{\partial w_{ij}} = \begin{cases} 1 & \text{if } \arg \min_{k \in \text{neighbors}(j)} (t_{c,k} + w_{kj}) = i \\ 0 & \text{otherwise} \end{cases}$$

If the LAT at point  $j$  is unknown, Eq. 2 is unrolled to the previous layers through the chain rule:

$$\frac{\partial \mathcal{L}}{\partial t_{c,j}} = \sum_{k \in \text{neighbors}(j)} \frac{\partial \mathcal{L}}{\partial t_{c,k}} \frac{\partial t_{c,k}}{\partial t_{c,j}}$$

with

$$\frac{\partial t_{c,k}}{\partial t_{c,j}} = \begin{cases} 1 & \text{if } \arg \min_{i \in \text{neighbors}(k)} (t_{c,i} + w_{ki}) = j \\ 0 & \text{otherwise} \end{cases}$$

and so on until the activation points are reached.

Once the edge weights are estimated, the point-wise conduction velocities  $c_i$  are derived. When both edge extremities belong to the same tissue type,  $c_i$  and  $c_j$  are trivially obtained. In the case they belong to different tissue types, the problem becomes ill-posed. To address this challenge, we assume the ratio of conduction velocities between different tissue types stays constant throughout the heart. The ratios are obtained directly from the initial personalization ( $c_{LV}/c_{RV}$ ,  $c_{LV}/c_{Myo}$  and other combinations, including scar and border zone when available). As an example, let point  $i$  belongs to LV endocardium and point  $j$  belongs to myocardium,  $L$  the distance between  $i$  and  $j$ ,  $l$  the distance between  $i$  and the boundary between tissue types,  $c$  the estimated apparent conductivity along this edge and  $\rho$  the ratio  $c_j/c_i$ . In this case, we have:

$$c_i = \frac{\rho l + (L - l)}{\rho L} c, \quad c_j = \rho c_i \quad (3)$$

Because each edge is processed independently, one vertex may have several estimated conduction velocities. In this case, the average value is taken and clamped within a physiological range for stability.

### 3 Experiments and Results

**Data Acquisition Protocol.** 16 pigs (average weight = 34 (30/35) kg) were studied, a sub-set of a larger database [9]. A left bundle branch block (LBBB) was induced in all animals using radio-frequency ablation. A cardiac resynchronization therapy (CRT) device was then positioned in the animal model. The RV lead was placed at the apex while the LV lead was positioned through a lateral or antero-lateral position of the LV epicardial surface. All pigs received an MRI a week before the experiment. LV endocardial and epicardial EAMs were acquired on the day of the experiment after LBBB (hereafter referred to as baseline), and with CRT pacing. An example of the data from these pig experiments is shown in Fig. 3. In all our experiments, both endocardial and epicardial EAMs were used. With respect to the gradient method, in all cases we used a stopping criteria of 0.01 ms in the activation time fitting. The maximum number of iterations allowed was 30 for the dense GraphEP personalization. All cases were observed to converge within this number of iterations.

**Verification on Synthetic Data.** The proposed GraphEP personalization method was first evaluated on synthetic data with known conductivity. The forward model was used to calculate “ground-truth” point-wise LAT on the endocardial and epicardial surface. Nine different distribution patterns of conductivity and LAT were generated (Fig. 2). First, conduction velocities were set within the endocardium layer prescribing the Purkinje network by (1) linearly varying conductivity values along the X, Y and Z axis of the anatomy within the interval [1.5, 4.0] m/s (3 models), (2) random velocities per American Heart Association (AHA) regions, within the same range (3 models), and (3) 10 random regions defined using region growing around random seeds (3 models). The endocardial conduction velocity was then propagated throughout the myocardium by assuming a constant Purkinje/myocardial cells ratio of 3. This procedure was repeated on two heart meshes generated from two different pigs, resulting in a total of 18 synthetic datasets. Finally, a virtual CRT was performed by placing an RV and LV electrode at standard location to test the predictive power of the personalized model.

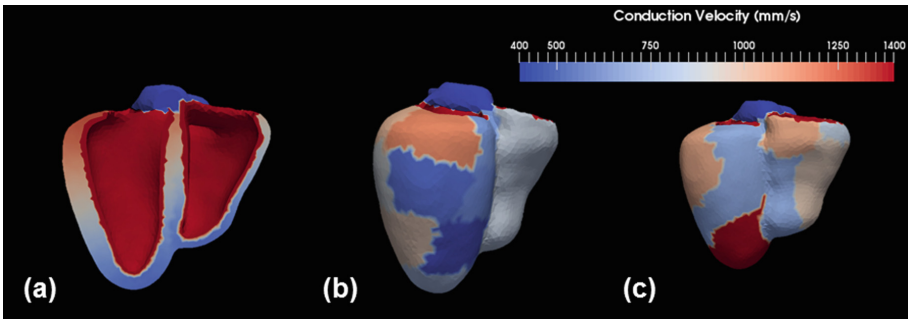


**Fig. 2.** Conductivity distribution of the synthetic datasets with (a) linearly varying distribution along the Y axis, (b) distribution according to AHA regions, and (c) region-growing regions based on random seeds.

The computed activation times normalized with respect to the simulated QRS duration is reported for both global and local personalization in Table 1. The proposed estimation method effectively estimated the ground truth conductivities, yielding an LAT error of less than 1 ms in average, compared with 4 ms for a global personalization. In all experiments, over-fitting was not severe since the CRT prediction was also significantly more accurate with locally estimated conductivities ( $1.3 \pm 0.4$  vs.  $6.2 \pm 2.6$  normalized AT error respectively). Interestingly, the performance of the proposed method was relatively insensitive to the distribution of conduction velocities, as highlighted by the min and max normalized LAT errors calculated as in Eq. 1. (Table 1).

**Table 1.** LAT errors between computed and ground truth on synthetic datasets, normalized with respect to QRS duration. For both baseline and CRT, the proposed local personalization yielded significant improvements in terms of accuracy (paired t-test,  $p < 0.5$ , values reported as mean  $\pm$  SD (min, max)).

	Global	Local
Baseline	$4.4 \pm 1.4(2.4, 7.2)$	$0.6 \pm 0.2(0.2, 1.2)$
CRT	$6.2 \pm 2.6(1.9, 11)$	$1.3 \pm 0.4(0.8, 2)$

**Evaluation on Animal Data for Cardiac Resynchronization Therapy.**

The result of the personalization after the global initialization and after the local refinement are compared. Both endo- and epi-cardial measured EAMs were used. The baseline and CRT simulation errors compared to the measurements for all pigs are presented in Table 2, with example visualizations of measured and simulated activation maps shown in Fig. 3. The results confirmed the trend observed in synthetic data. Table 2 shows that the proposed local estimation method consistently resulted in lower mean LAT error across the whole heart and also when considering each ventricle individually, in the case of both baseline rhythm and after CRT. It is also interesting to note the lower standard deviation of LAT errors for the proposed method, which points toward the improved ability to accurately personalize local variations in conductivity across the heart. In both the global and local personalization methods, the residual error was consistently higher for CRT than the baseline. This reflects the complexity of accurately modeling all of the parameters involved in CRT, such as lead placement, which could only be approximated from the EAMs as the center of the early activation areas. It is especially important to note that the QRS length at baseline LBBB was measured to be on average  $46.6 \pm 18.3$ ms, and after CRT was found to be  $70.3 \pm 14.0$  ms (in some animals, the electrodes were not placed optimally). As a result, the simulated LAT errors were below the activation difference in pre/post-CRT.

**Computation time.** In this experiment, a personalization took less than one minute without code optimization on a tetrahedral mesh of approximately 14,000 vertices using a standard laptop (Intel Core i7-4800MQ 2.70 GHz, 8 GB of RAM), owing to the fast graph-based algorithms.

**Table 2.** Absolute LAT errors (in ms) for baseline and CRT simulations in the swine dataset. Values reported as mean  $\pm$  SD, per ventricle and over the entire bi-ventricular myocardium. Goodness of fit and predictive power significantly improved after local personalization.

	Global			Local		
	WholeHeart	LV	RV	WholeHeart	LV	RV
Baseline	$12.2 \pm 5.2$	$8.8 \pm 4.0$	$11.8 \pm 5.3$	$3.7 \pm 1.7$	$4.8 \pm 2.0$	$2.0 \pm 0.9$
CRT	$14.8 \pm 6.6$	$24.4 \pm 11.7$	$25.8 \pm 12.0$	$10.0 \pm 4.5$	$15.4 \pm 6.7$	$17.8 \pm 8.1$

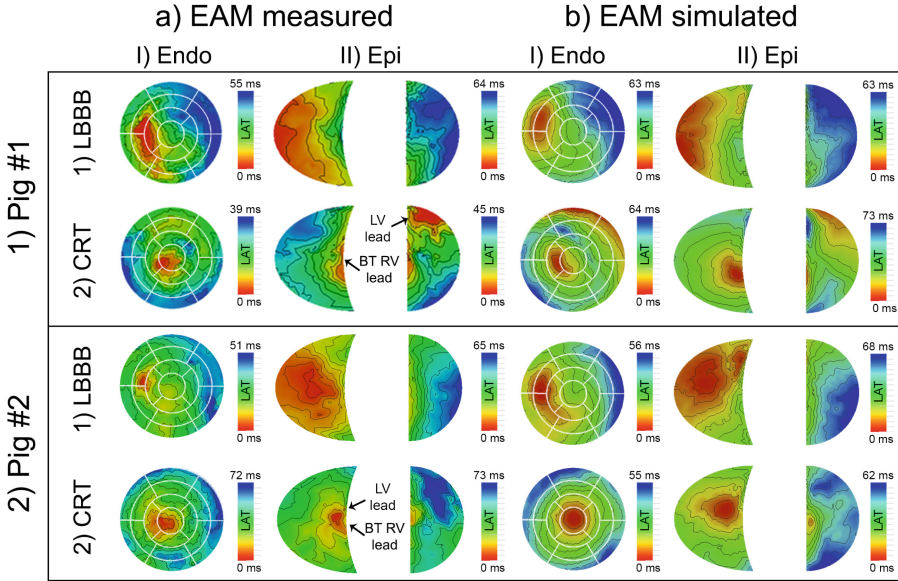


**Fig. 3.** Example data from two pigs showing the measured EAMs during baseline LBBB rhythm and CRT activation, with the corresponding simulated EAMs using the proposed local personalization of conductivity. The approach yielded qualitatively similar maps at baseline and during CRT, suggesting a good fit to the data.

## 4 Discussion and Conclusion

This paper presented a novel method to estimate the electrical conduction velocity at every point of the myocardium. The proposed method has a number of advantages. It allows personalization of heart activation patterns to the resolution of the computational domain mesh, while being extremely computationally efficient. The method is also adaptable to varying levels of sparsity in the measured LAT input values. However, one disadvantage of using a variant of back-propagation is the potential over-fitting of the model. Yet, the obtained CRT predictions suggest predictions are still much more precise with the proposed method than with global estimation. Further investigation is needed to evaluate the sensitivity of the method to noise and missing data. Possible future directions are to incorporate prior knowledge of the heart conduction pathways to regularize the personalization, add measurement uncertainty to the estimation process, and further validate the approach.

**Disclaimer:** This feature is based on research, and is not commercially available. Due to regulatory reasons its future availability cannot be guaranteed.



## References

1. Arevalo, H.J., Vadakkumpadan, F., Guallar, E., Jebb, A., Malamas, P., Wu, K.C., Trayanova, N.A.: Arrhythmia risk stratification of patients after myocardial infarction using personalized heart models. *Nat. Commun.* **7** (2016)
2. Bayer, J.D., Roney, C.H., Pashaei, A., Jaïs, P., Vigmond, E.J.: Novel radiofrequency ablation strategies for terminating atrial fibrillation in the left atrium: a simulation study. *Front. Physiol.* **7**, 108 (2016)
3. Chabiniok, R., Wang, V.Y., Hadjicharalambous, M., Asner, L., Lee, J., Sermesant, M., Kuhl, E., Young, A.A., Moireau, P., Nash, M.P., et al.: Multiphysics and multiscale modelling, data-model fusion and integration of organ physiology in the clinic: ventricular cardiac mechanics. *Interface Focus* **6**(2), 20150083 (2016)
4. LeCun, Y., Bengio, Y., Hinton, G.: Deep learning. *Nature* **521**(7553), 436–444 (2015)
5. Marchesseau, S., Delingette, H., Sermesant, M., Cabrera-Lozoya, R., Tobon-Gomez, C., Moireau, P., I Ventura, R.F., Lekadir, K., Hernandez, A., Garreau, M., et al.: Personalization of a cardiac electromechanical model using reduced order unscented kalman filtering from regional volumes. *MedIA* **17**(7), 816–829 (2013)
6. Neumann, D., Mansi, T., Itu, L., Georgescu, B., Kayvanpour, E., Sedaghat-Hamedani, F., Amr, A., Haas, J., Katus, H., Meder, B., et al.: A self-taught artificial agent for multi-physics computational model personalization. *MedIA* **34**, 52–64 (2016)
7. Powell, M.J.: The bobyqa algorithm for bound constrained optimization without derivatives. Cambridge NA Report NA2009/06, University of Cambridge, Cambridge (2009)
8. Relan, J., Chinchapatnam, P., Sermesant, M., Rhode, K., Ginks, M., Delingette, H., Rinaldi, C.A., Razavi, R., Ayache, N.: Coupled personalization of cardiac electrophysiology models for prediction of ischaemic ventricular tachycardia. *Interface Focus* **1**, 396–407 (2011)
9. Rigol, M., Solanes, N., Fernandez-Armenta, J., Silva, E., Doltra, A., Duchateau, N., Barcelo, A., Gabrielli, L., Bijmens, B., Berruezo, A., et al.: Development of a swine model of left bundle branch block for experimental studies of cardiac resynchronization therapy. *JCTR* **6**(4), 616–622 (2013)
10. Sermesant, M., Chabiniok, R., Chinchapatnam, P., Mansi, T., Billet, F., Moireau, P., Peyrat, J.M., Wong, K., Relan, J., Rhode, K., et al.: Patient-specific electro-mechanical models of the heart for the prediction of pacing acute effects in crt: a preliminary clinical validation. *MedIA* **16**(1), 201–215 (2012)
11. Sermesant, M., Moireau, P., Camara, O., Sainte-Marie, J., Andriantsimiavona, R., Cimrman, R., Hill, D.L., Chapelle, D., Razavi, R.: Cardiac function estimation from mri using a heart model and data assimilation: advances and difficulties. *MedIA* **10**(4), 642–656 (2006)
12. Sohal, M., Shetty, A., Niederer, S., Lee, A., Chen, Z., Jackson, T., Behar, J.M., Claridge, S., Bostock, J., Hyde, E., et al.: Mechanistic insights into the benefits of multisite pacing in cardiac resynchronization therapy: the importance of electrical substrate and rate of left ventricular activation. *Heart Rhythm* **12**(12), 2449–2457 (2015)
13. Soto-Iglesias, D., Butakoff, C., Andreu, D., Fernández-Armenta, J., Berruezo, A., Camara, O.: Integration of electro-anatomical and imaging data of the left ventricle: an evaluation framework. *MedIA* **32**, 131–144 (2016)

14. Wallman, M., Smith, N.P., Rodriguez, B.: A comparative study of graph-based, eikonal, and monodomain simulations for the estimation of cardiac activation times. *IEEE Trans. Biomed. Eng.* **59**(6), 1739–1748 (2012). <http://ieeexplore.ieee.org/document/6178774/>
15. Wallman, M., Smith, N.P., Rodriguez, B.: Computational methods to reduce uncertainty in the estimation of cardiac conduction properties from electroanatomical recordings. *MedIA* **18**(1), 228–240 (2014)